

Central European Journal of Chemistry

Surface enhanced raman scattering of aromatic thiols adsorbed on nanostructured gold surfaces

Research Article

Mamdouh E. Abdelsalam

Department of Chemistry, Faculty of Science, Tanta University, 31527-Tanta, Egypt

Received 19 October 2008; Accepted 07 January 2009

Abstract: In this paper we describe the use of a simple and versatile technique of templated electrodeposition through polystyrene sphere templates to produce nanostructured films of gold with regular submicron spherical holes arranged in a hexagonal close-packed structure. The templates were produced by self assembly of a monodispersed suspension of polystyrene spheres on gold substrates using capillary forces. The self assembly process was modified through the chemical modification of the gold substrate with cysteamine thiol. Films of gold were prepared by electrochemical deposition through the template. The electrochemical deposition charge and the current time curve were used to control the film height with a precision of approximately 10 nm. The colour of the nanostructured films

time curve were used to control the film height with a precision of approximately 10 nm. The colour of the nanostructured films changed as the film thickness was changed. Surface enhanced Raman Scattering spectra were recorded and used to identify very low concentrations of aromatic thiol molecules, 4-Nitrobenzenethiol (4-NBT) and 4-Aminobenzenethiol (4-ABT), adsorbed on the surface of the nanostructured gold substrates.

Keywords: Templated electrodeposition • Nanostructured gold • SERS, 4-Nitrobenzenethiol • 4-Aminobenzenethiol

© Versita Warsaw and Springer-Verlag Berlin Heidelberg.

1. Introduction

Fabrication of nanostructured materials have recently attracted much attention due to their unique properties which are superior to those of bulk materials [1-2]. Templated-deposition techniques have been widely used to fabricate nanostructured materials at a very low cost. First, the template is assembled from a self-organizing material. Submicron size polystyrene spheres have become widely used materials to assemble the templates because they are commercially available in a wide range of sizes with narrow size distribution [3]. Several methods, e.g. gravity sedimentation [4-6] and capillary force at a meniscus between a substrate and the spheres colloidal solution [7-11], were used for assembling the spheres into templates. After the formation of the templates, the interstitials spaces are then impregnated with the desired precursors. Finally, the template is removed, resulting in arrays of nanoporous films that reflect the structure of the template. Nanoporous films have been prepared by several groups by infiltration of the spaces

between the template by metals [8,12-13], metal oxides [14-15], metal alloys and polymers [17-18].

Nanostructured materials have been used in wide applications as electrocatalysts [19-20], sensors [21], filters [22-23] and Surface Enhanced Raman Scattering (SERS) substrates [24-26]. SERS has a number of attributes which make it a very attractive technique for investigating molecules adsorbed on surfaces. Firstly, the surface enhancement is highly selective so the technique is sensitive to molecules adsorbed at, or very close to, the surface and it thus discriminates against molecules in the bulk solution. Secondly, SERS gives information about the molecular structure of the adsorbate, including its orientation at the surface [27-28]. Finally, the Raman cross section for water is low so that SERS can be easily used to study electrodes in aqueous solution.

In this paper we describe a simple and versatile technique of templated electrodeposition to fabricate nanostructured gold surfaces with controllable geometries. The templates were produced by self

assembly of a monodispersed suspension of polystyrene spheres on gold substrates using capillary forces. Films of gold were prepared by electrochemical deposition through the template. The electrochemical deposition charge was used to control the film height. Because the templated electrodeposition technique enabled us to precisely tailor the gold electrodes and therefore to tune the surface plasmon modes to match the requirements of SERS experiment. These gold electrodes have been used as SERS active substrates with significant signal enhancements to identify molecules absorbed on their surfaces.

2. Experimental Procedures

2.1 Materials and solutions

The monodisperse polystyrene latex spheres, with diameters of 200 nm ± 5 nm and 1 µm ± 7 nm were obtained from Brookhaven as a 1 wt% solution in water with coefficient of variation in diameter of 1.3%. 4-Nitrobenzenethiol (4-NBT), 4-Aminobenzenethiol tetrahydrofuran (4-ABT), isopropanol, (THF). cysteamine, and ethanol were obtained from Aldrich. The gold substrates were prepared by evaporating 10 nm of a chromium adhesion, followed by 200 nm of gold, onto 1 mm thick glass microscope slides. The gold substrates were thoroughly cleaned before used. First it was sonicated in deionised water for 30 minutes followed by sonication in isopropanol for 90 minutes then rinsed with deionized water. Finally the substrate was dried under a pure and gentle argon stream and was used directly. All solvents and chemicals were of reagent quality and were used without further purification. All solutions were freshly prepared using reagent-grade water (18 MΩ cm) from a Whatman RO80 system coupled to a Whatman "Still Plus" system.

The gold substrates were chemically modified with cysteamine. The latter was self-assembled by immersing the cleaned gold substrate in a 10 mM ethanolic solution of cysteamine at room temperature for three days. Self-assembled monolayers (SAM) of cysteamine were characterized by measuring the contact angle for the gold substrate before and after treating with the thiol solutions. Contact angles were determined using a purpose built arrangement assembled on a vibrationally isolated platform. Measurements were made in a sealed glass chamber at 100% humidity. Polystyrene sphere templates were self assembled on clean and modified gold substrates in a thin layer cell, details regarding the thin layer cell arrangement and contact angle measurements have been previously reported [13,29].

Electrochemical deposition of gold films was carried out from a cyanide free gold plating solution containing 7.07 g dm³ gold (Tech. Gold 25, Technic Inc. Cranston, RI) using a conventional three-electrode cell controlled by an Autolab Potentiostat/Galvanostat Model PGSTAT30 under potentiostatic conditions at -0.7 V vs. saturated calomel electrode (SCE) as reference electrode at 25°C. After deposition the samples were soaked in THF for two hours to remove the polystyrene template. In some experiments gold films were grown with a series of steps of various thicknesses. This was achieved by withdrawing the substrate in a series of steps (each of about 500 μ m) from the electrodeposition solution using a microstage.

2.2 Instrumentation

An environmental scanning electron microscope, SEM, (Philips XL30 ESEM) was used to study the morphology and structure of both the polystyrene templates and the metal films. The optical images of the nanostructured films were measured using an optical microscopy arrangement (BX51TRF Olympus) using a white light source to illuminate the samples. Images were recorded using a CCD camera (DP2 Olympus). All Raman spectra were recorded on a Renishaw Raman 2000 system using a 633 nm HeNe laser with 5 µm diameter spot size and 3 mW power using a single 10 s accumulation.

3. Results and discussion

3.1 Chemical modification of gold substrates

Cysteamine was self-assembled on gold substrates by immersing the freshly cleaned substrates in a 10 mM ethanolic solution of cysteamine at room temperature for three days. The SH group of the thiol molecules adsorb readily from solution onto the gold, creating a dense monolayer. Modifying the gold substrate with cysteamine has two effects. First, it increases the efficiency of the assembly of the polystyrene spheres on the gold substrate by increasing the substrate-particles interaction. This is because the substrate surface is positively charged as results of the chemical modification with the cysteamine and the spheres have a negative surface charge due to the sulphate groups used to stabilize the polystyrene suspension [30]. Second, it increases the wettability of the gold substrate. We found that the contact angle for the drop of water changed from 70° to 40° for gold surface before and after treating with cysteamine. This significant increase in the wettability assists the formation of a thin meniscus between the spheres and the substrate, which is necessary for the self-assembly of the templates.

3.2 Self-assembly of templates

Recently, the strong capillary forces which develop at a meniscus between a substrate and a colloidal solution have been used to produce thick templates of three dimensional arrays [7-11]. A modification of this approach was used in the present work using cysteamine modified gold surfaces which greatly enhances the assembly of the template. The formation of templates of polystyrene spheres on the modified gold surface was achieved by careful control of the evaporation rate of the spheres suspended in water. The arrangement of the spheres in the template films was investigated using high magnification scanning electron microscopy. Fig. 1 shows SEM images of a typical template assembled from 500 nm polystyrene spheres on a cysteamine treated gold surface. The spheres are close packed in a well ordered hexagonal array. Apparently the layers of template are oriented with their axes parallel to the

substrate. One of the great advantages of the templates formation method reported herein is the ability to create samples with controlled thickness. This was achieved by controlling such parameters as the sphere concentrations, the thickness of the thin layer cell and the ability to repeat the assembly step. It was possible to vary the thickness of the templates from a single monolayer (Fig. 1a), two layers (Fig. 1b), seven layers (Fig. 1c) and up to fifteen layers (Fig. 1d).

After drying the template appears opalescent with colures changing from green to red, depending on the angle of observation, clearly visible when illuminated from above with white light. The templates are robust and adhere well to the gold substrates. We normally leave the templates in the electroplating solutions for 20 min before applying the potential required for the electro deposition. This time is to give the metal ions a chance to diffuse in the interstitial spaces between the spheres.

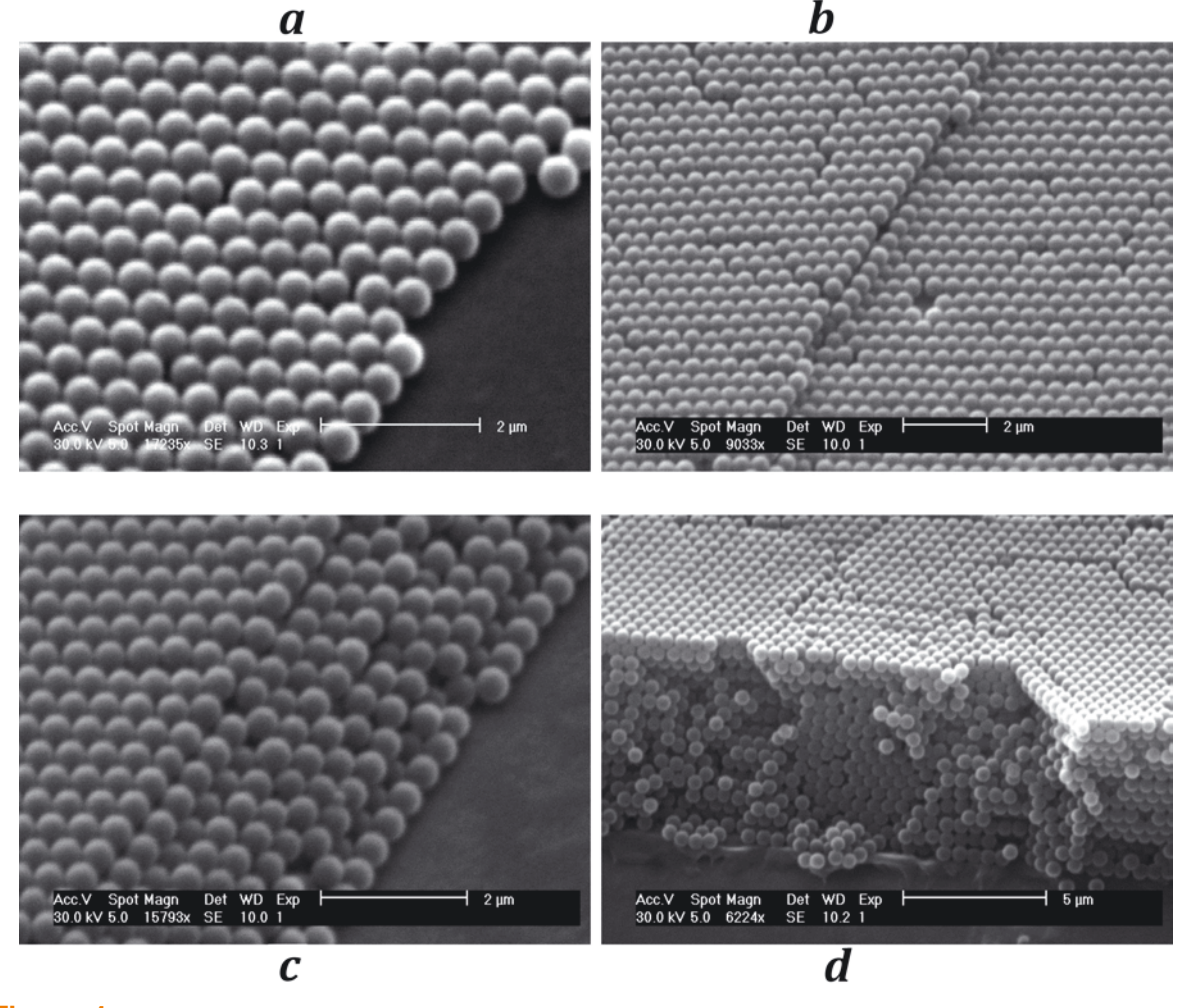


Figure 1. SEM images of templates made from polystyrene spheres of 500 nm diameter and have different number of layers (a) monolayer, (b) two layers, (c) 7 layers and (d) 15 layers.

This added to the time taken during the electrochemical deposition. Despite this long contact time being the template and electroplating solution, there was no evidence of their re-suspension in the solutions.

3.3 Electrochemical deposition

Gold films of controlled thickness were electrochemically deposited from aqueous solution through the potentiostatic pre-assembled templates, under conditions at -0.7 V vs. SCE. Fig. 2a-d shows the current vs. time curves together with SEM images for films grown up to various thicknesses of 1/4, 1/2, 3/4 and 1 of the sphere diameter respectively. The plating films were electrodeposited through a template of single 1000 nm diameter monolayer of polystyrene spheres. During the electrodeposition of gold through the template we observed temporal oscillations in the current, which allowed us to control the thickness of nanostructured gold with a precision of approximately 10 nm. These oscillations can be explained by the periodic variation of the active electrode surface area during the growth of the gold in the template. At the beginning of the deposition each polystyrene sphere of the template is in contact with the electrode surface at only one point, and therefore both the electrode surface

and the deposition current are maximal (Fig. 2a). As the gold grows around the template, the active electrode surface area decreases continuously and goes through a minimum (Fig. 2b) when the metal thickness reaches the middle of the monolayer of spheres because the particles are touching each other at this level. The current then increases as the film grows beyond this point and the active electrode area increases (Fig. 2c-d). Oscillations of this kind have been observed by others [31]. In the present case the oscillations are extremely high in amplitude and give us an easy and reliable way to control the film thickness. The thickness of the electrodeposited film was precisely controlled by varying the charge passed during electrodeposition and watching the shape of current time curves.

Film thicknesses were also calculated using the radius of the pore mouth measured in the SEM and the known radius of the template sphere. From simple trigonometry the thickness is given by [13]:

$$t = r \pm (r^2 - r_{\text{pore}}^2)^{1/2} \tag{1}$$

where t is the film thickness, r the radius of the template sphere and $r_{\rm pore}$ the radius of the pore mouth. The choice sign for the \pm term depends on whether the film is thicker

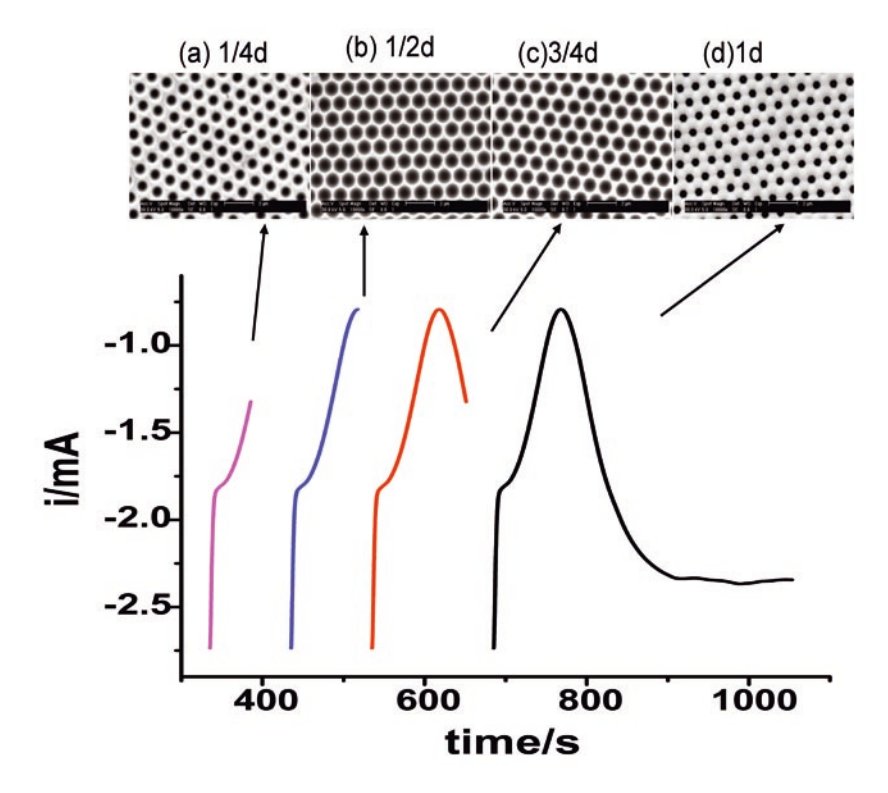


Figure 2. Current-time curves together with corresponding SEM images for gold templated films made using polystyrene spheres of 1000 nm diameter. The Electrodeposition potential was – 0.7 V vs. SCE. The films have different thickness of (a) 1/4d; (b) 1/2d; (c) 3/4d and (d) 1 d, where is d is the sphere diameter. The individual i-t curves are off-set for clarity.

or thinner than the radius of the template sphere. Good agreement between the film thickness obtained from the current time curve and that calculated using Eq. 1 was obtained.

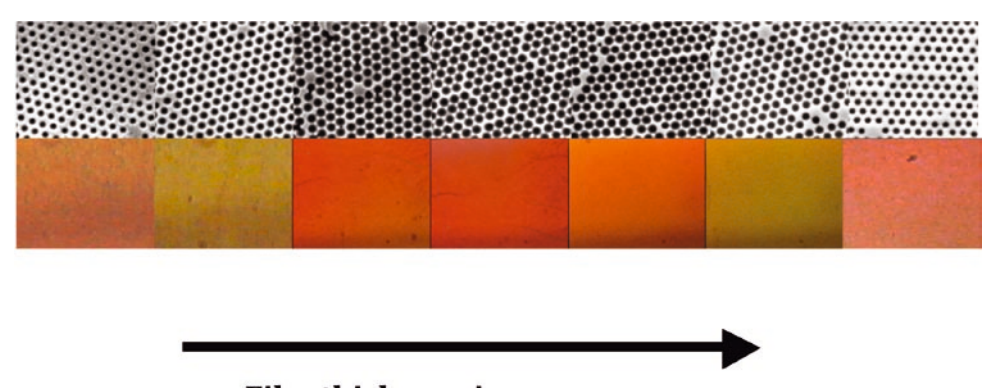
To grade the thickness of the deposited film, the sample is mounted on a micrometer stage, allowing the systematic retraction of the surface out of the plating bath. Fig. 3 shows SEM images together with corresponding optical images for nanostructured films of gold grown through a monolayer template of 500 nm of polystyrene spheres. Films were grown with a series of steps in thickness by withdrawing the substrate in a series of steps (each $\sim 500~\mu m)$ from the solution during electrodeposition. At every step the new plating area is measured, allowing the absolute thickness of each deposited step to be calculated. After deposition the samples are washed in THF to remove the latex spheres.

The optical images show the striking range of colors of the film when viewed at normal incidence, changing from green through red, orange and then back to green as the film thickness increases from 0 to 1D. The corresponding SEM images show the associated change in pore mouth diameter. Because the pore diameters of the nanostructured films correspond to the wavelength of visible light, these metal films exhibit optical diffraction phenomena that lead to striking optical properties. It is clearly evident that the film color varies with the film thickness indicating that the precise geometry of the structured film is an important factor in controlling the optical properties. These results agree with what have been reported previously for nanostructured Pt and Pd substrates [25]. The change in color is attributed to the surface and the localized Plasmons modes associated with the change in the topology of the nanostructured films as the film height changes; this have been previously discussed [13,25,32].

3.4 SERS spectra for 4-NBT and 4-ABT

SERS spectra were recorded and used to identify aromatic thiol molecules adsorbed on the surface of the nanostructured gold substrates. 4-NBT and 4-ABT were adsorbed on the gold surfaces by soaking in a 10 mM solution in ethanol for 10 min. The samples were then rinsed with ethanol, and left to dry in air for 15 min before measurement. Fig. 4a shows the SERS spectrum of 4-NBT adsorbed on a structured gold surface, (thickness 450 nm, 600 nm template sphere diameter). The band positions and relative intensities observed in the SERS spectra for 4-NBT on gold agree well with those in the literature [33-34]. The complete absence of the S-H stretching peak in the SERS spectrum, observable at 2548 cm⁻¹ for pure 4-NBT (not shown in these Figures), indicates that 4-NBT is adsorbed on gold as thiolate after S-H bond cleavage. All of the peaks in Fig. 4a can then be attributed to 4-NBT. The prominent peak around 1343 cm⁻¹ is due to the symmetric stretching vibration of the nitro group of 4-NBT [v(NO₂)]. Moreover well defined peaks are observed for the ring stretching and bending at 1573 and 1002 cm⁻¹, the C-H bending and stretching at 1180, 1111 and 1032 cm-1 and C-H wagging at 856 cm⁻¹. Full assignment of SERS peaks for the adsorbed 4-NBT is summarized in Table 1.

Fig. 4b shows the SERS spectrum of 4-ABT adsorbed on the surface of a nanostructured gold film (thickness 450 nm, 600 nm template sphere diameter). The band positions and relative intensities agree well with those values found in the literature [34-35] . The spectra are dominated with the stretching modes, such as v(CC) and v(CS) at 1577 and 1076 cm⁻¹ respectively. Importantly, the stretching and bending modes located at 1434 and 1387 cm⁻¹ can also be clearly observed. The full assignment of SERS peaks for the adsorbed 4-ABT is summarized in Table 1.



Film thickness increase

Figure 3. SEM images and the corresponding optical images for a graded, nanostructured gold film grown through a 500 nm sphere diameter template. The arrow shows the direction of the increasing of the film thickness.

Table 1. SERS peak assignment of 4-NBT and 4-ABT on nanostructured gold substrates.

SERS peak (cm ⁻¹)		Assignment ^a
4-NBT	4-ABT	
1573s	1577	ν(CC)
	1434	$\nu(CC) + \delta(CH)$
	1387	$\nu(CC) + \delta(CH)$
1343		v(NO2)
	1307	
1180	1190	ν(CH)
	1142	ν(CH)
1111		δ(CH)
1082	1076	ν(CS)
1032		δ(CH)
1002	1007	$\gamma(CC) + \gamma(CCC)$
856		π(CH)

v, stretch; δ and γ, bend; and π, wagging.

Both spectra in Fig. 4 show well defined SERS peaks with significant enhancement in the intensity as indicated by the high signal to noise ratio. This results agree very well with our pervious results obtained for benzenethiol adsorbed on nanostructured Pt and Pd substrates [24-25,32]. Fig. 4 shows the most intense SERS spectra for adsorbed 4-NBT and 4-ABT obtained using a 633 nm excitation laser for graded in thickness gold samples.

We found that, the SERS enhancement depends on the geometry of the structured films. In pervious studies [24-25], to relate the dependence of the SERS enhancement to the geometry of the structured film, we recorded reflectance spectra for gold surfaces as a function of film thickness at the same positions on the graded substrates at which the SERS were measured. Dips in reflectivity, corresponding to localized plasmon absorption, are observed which shift to progressively longer wavelength as the film thickness increases, causing dramatic changes in the observed color of the sample similar to what is shown in Fig. 3 in this paper. We attributed the dips in the reflectance spectra to the relative contributions of surface (Bragg) plasmons and localised (Mie) plasmons modes [36]. When the film is very thin the surface takes the form of an array of shallow dishes, ordered in a close packed hexagonal lattice, with the top surfaces consisting of flat areas of metal separating the dishes. Plasmons freely propagate on the flat surface and multiply scatter off the rims of the dishes resulting in plasmonic band gaps following Bragg dispersion [37]. As the film thickness increases the surface becomes strongly corrugated, and in addition to the (Bragg) surface plasmons travelling across the top surface, other plasmons are trapped within the spherical cavities. For fully spherical cavities, i.e. if the top surface were to close over, these trapped plasmons may be

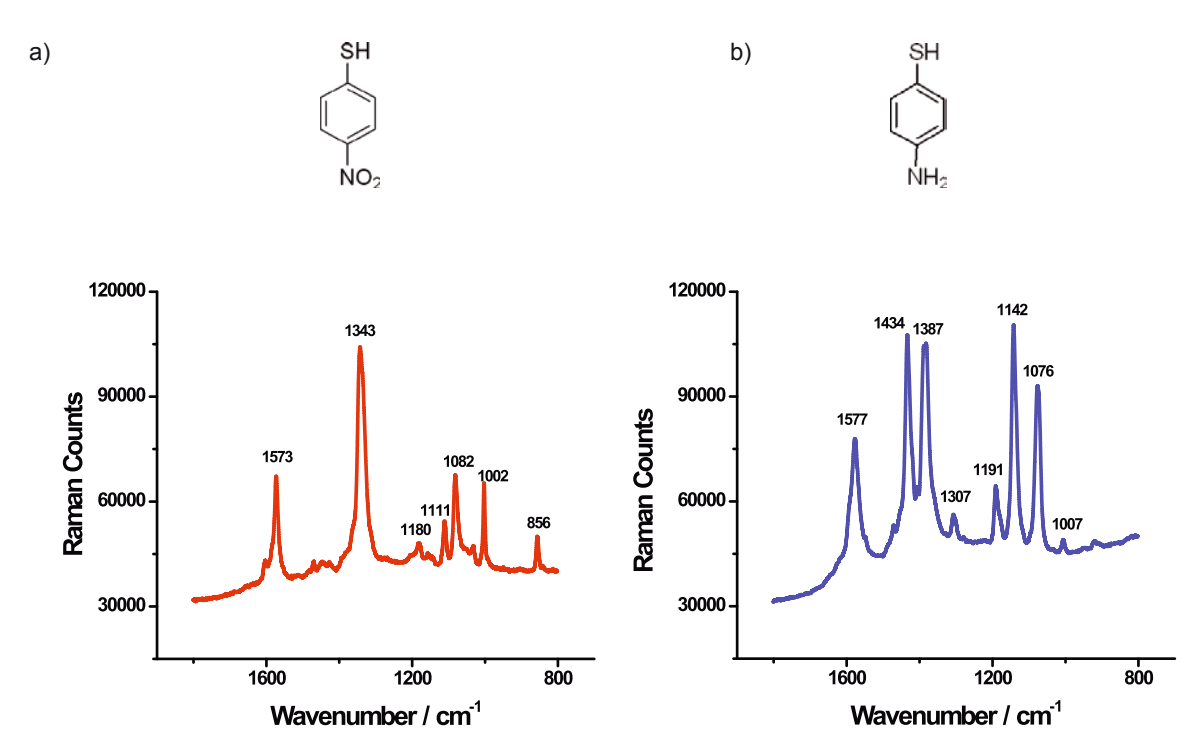


Figure 4. SERS spectrum of (a) 4-NBT and (b) 4-ABT adsorbed on a templated gold film produced using 600 nm polystyrene spheres and grown to a thickness of 450 nm. The spectrum was taken using 633 nm HeNe laser, 3 mW power, single 10 s accumulation.

^a Assignment made by consulting refs [33-35]

modelled using Mie scattering and, therefore, they have described as Mie modes. The Mie and Bragg modes interfere with the incoming light and this interference produces series of dips in the reflectance spectra of the films. In recent studies we have used angle-resolved reflectivity measurements of templated gold films to allow us to fully map the spectral and angular dispersion of the different types of plasmons and their interactions [38]. Moreover we were able to map the SERS signal intensity at different angles of both the incident pump laser and the Stokes scattered photons and thus clearly demonstrated the role of resonant plasmon enhancement for both incoming and outgoing light on the SERS signal intensity [32]. Sharp enhancements occur when the laser is scanned through a plasmon resonance (ingoing) and also when individual Raman scattered lines coincide with plasmon resonances (outgoing). Consequently, to achieve maximal surface enhancement templated substrates have to be carefully designed bearing in mind not only the wavelength of the exciting laser but also the geometry of the substrate. For the 600 nm sphere templated gold films used to record the spectra shown in Fig. 4, both the wavelength of the excitation laser and the Stokes scattered photons overlap with a strong absorption features in the reflectance spectra for a film height of 3/4 the sphere diameter (450 nm). A more detailed analysis is beyond the scope of the present paper and have been discussed in details in earlier publications [24,36,38].

Comparing the spectrum for 4-NBT with the spectrum for 4-ABT, many difference can be identified. First, the very strong peak obtained at 1134 cm⁻¹ for 4-NBT is considered a signature for the 4-NBT due to the symmetric stretching of the NO₂ group. Second, the presence of the very strong stretching peaks at 1434 and 1387 cm⁻¹ only in the 4-ABT spectrum are attributed to the ring stretching and bending modes. Two thiols molecules that have been investigated show that, aside from the NO₂ and NH₂ groups at position 4, they have the same molecular structure but the SERS spectra are different. Therefore the combination of the SESR with

nanostructured gold electrodes provides an excellent and powerful method to identify very low concentrations of the adsorbed molecules on their surfaces. Moreover, the nanostructured gold substrate reported in this paper is very stable and can be used several times provided it is subjected to cleaning before use. The chemical and electrochemical stability of the substrates make it a very good candidate for the electrochemical SERS applications [39].

4. Conclusion

In this study we have shown that the templated electrodeposition technique can be used to produce gold films that give SERS active substrates with significant signal enhancements. An advantages of the structured surfaces reported here is that both the template sphere diameter and the film thickness can be varied to allow control over the optical properties of the substrates. The surfaces can therefore be precisely tailored to tune the surface plasmon modes to match the requirements of SERS experiment. The maximum surface enhancement was obtained when the incident and Stokes scattered radiation match plasmonic resonance of the surface. Nanostructured gold films reported in this paper were successfully used as SERS substrate. Well defined SERS spectra of 4-NBT and 4-ABT adsorbed on a structured gold surface were obtained.

Acknowledgment

The Author specially thanks Prof. Jeremy Baumberg (School of Physics and Astronomy, University of Southampton), Prof. Phil Bartlett and Prof. Andrea Russell (School of Chemistry, University of Southampton) for their great help and support during his work at the School of Chemistry, University of Southampton and thanks the EPSRC for funding.

References

- [1] C.B. Murray, C.R. Kagan, M.G. Bawendi, Science 270, 1335 (1995)
- [2] M. Zhao, L. Sun, R.M. Crooks, J. Am. Chem. Soc. 120, 4877 (1998)
- [3] M. Himmelhaus, H.Takei, Phys. Chem. Chem. Phys 4, 496 (2002)
- [4] P. Pieranski, Contemp. Phys. 24, 25 (1983)
- [5] K.E. Davis, W.B. Russel, W.J. Glantschnig, J. Chem. Soc., Faraday Trans. 87, 411 (1991)
- [6] H. Miguez, F. Meseguer, C. Lopez, A. Blanco, J.S. Moya, J. Requena, A. Mifsud, V. Fornes, Adv. Mater. 10, 480 (1998)
- [7] N.D. Denkov, O.D. Velev, P.A. Kralchevsky, I.B. Ivanov, H. Yoshimura, K. Nagayama, Nature 361, 26 (1993)

- [8] O.D. Velev, P.M. Tessier, A.M. Lenhoff, E.W. Kaler, Nature 401, 548 (1999)
- [9] K. Nagayama, Colloids Surf. 109, 363 (1996)
- [10] P. Jiang, J.F. Bertone, K.S. Hwang, V.L. Colvin, Chem. Mater. 11, 2132 (1999)
- [11] Y.A. Vlasov, X.-Z. Bo, J.C. Sturm, D.J. Norris, Nature 414, 289 (2001)
- [12] P.N. Bartlett, J.J. Baumberg, P.R. Birkin, M.A. Ghanem, M.C. Netti, Chem. Mater. 14, 2199 (2002)
- [13] P.N. Bartlett, J.J. Baumberg, S. Coyle, M.E. Abdelsalam, Farad. Discuss. 125, 117 (2004)
- [14] B.T. Holland, C.F. Blanford, T. Do, A. Stein, Science 281, 538 (1998)
- [15] J.E.G.J. Wijnhoven, W.L. Vos, Science 281, 802 (1998)
- [16] H. Yan, C.F. Blanford, W.H. Smyrl, A. Stein, Chem. Commun. 1477 (2000)
- [17] P. Jiang, K.S. Hawang, D.M. Mittleman, J.F. Bertone, V.L. Colvin, J. Am. Chem. Soc. 121, 11630 (1999)
- [18] S.A. Johnson, P.J. Ollivier, T.E. Mallouk, Science 283, 963 (1999)
- [19] P. Hoyer, Langmuir 14, 1411 (1996)
- [20] I. Moriguchi, H. Maeda, Y. Teraoka, S. Kagawa, Chem. Mater. 9, 1050 (1997)
- [21] R.W.J. Scott, S.M. Yang, G. Chabanis, N. Coombs, D.E. Williams, G.A. Ozin, Adv. Mater. 13, 1468 (2001)
- [22] S.H. Park, Y. Xia, Chem. Mater. 10, 1745 (1998)
- [23] S.H. Park, Y. Xia, Adv. Mater. 10, 1045 (1998)
- [24] S. Cintra, M.E. Abdelsalam, P.N. Bartlett, J.J. Baumberg, T.A. Kelf, Y. Suguwara, A.E. Russell, Farad. Discuss. 132, 191 (2006)
- [25] M.E. Abdelsalam, S. Mahajan, P.N. Bartlett, J.J. Baumberg, A.E. Russell, J. Am. Chem. Soc. 129, 7399 (2007)

- [26] S. Mahajan, M.E. Abdelsalam, Y. Suguwara, S. Cintra, A.E. Russell, J.J. Baumberg, P.N. Bartlett, Phys. Chem. Chem. Phys. 9, 104 (2007)
- [27] L.A. Dick, A.D. Mcfarland, C.L. Haynes, R.P. Van Duyne, J. Phys. Chem. B 106, 853 (2002)
- [28] Z.Q. Tian, B. Ren, D.Y. Wu, J. Phys. Chem. B 106, 9463 (2002)
- [29] M.E. Abdelsalam, P.N. Bartlett, T.A. Kelf, J.J. Baumberg, Langmuir 21, 1753 (2005)
- [30] G.W. Poehlein, R.H. Ottewill, J.W. Goodwin, Science and Technology of Polymer Colloids (Martinus Nijhoff Publishers, Boston, 1983)
- [31] R. Szamocki, S. Reculusa, S. Ravaine, P.N. Bartlett, A. Kuhn, R. Hempelmann, Angew. Chem., Int. Ed. Engl. 45, 1317 (2006)
- [32] J.J. Baumberg, T.A. Kelf, Y. Suguwara, S. Cintra, M.E. Abdelsalam, P.N. Bartlett, W.B. Russel, Nano Lett. 5, 2262 (2005)
- [33] B.O. Skadtchenko, R. Aroca, Spectrochimica Acta, Part A 57, 1009 (2001)
- [34] K.S. Shin, H.S. Lee, S.W. Joo, K. Kim, J. Phys. Chem. C 111, 15223 (2007)
- [35] J. Zheng, Y. Zhou, X. Li, Y. Ji, T. Lu, R. Gu, Langmuir 19, 632 (2003)
- [36] T.A. Kelf, Y. Sugawara, J.J. Baumberg, M.E. Abdelsalam, P.N. Bartlett, Phys. Rev. Lett. 95, 116802 (2005)
- [37] W.L. Barnes, A. Dereux, T.W. Ebbesen, Nature 424, 824 (2003)
- [38] T.A. Kelf, Y. Sugawara, R.M. Cole, J.J. Baumberg, M.E. Abdelsalam, S. Cintra, S. Mahajan, A.E. Russell, P.N. Bartlett, Phys. Rev. B 74, 245415 (2006)
- [39] M.E. Abdelsalam, P.N. Bartlett, J.J. Baumberg, S. Cintra, T.A. Kelf, A.E. Russell, Electrochem. Commun. 7, 740 (2005)